MDPI

Changing Water Cycle under a Warming Climate: Tendencies in the Carpathian Basin

Imre Miklós Jánosi [1,2,*,†] , Tibor Bíró [3,†] , Boglárka O. Lakatos [4,5,†] , Jason A. C. Gallas [2,6,†] and András Szöllősi-Nagy [1,†]

1   Department of Water and Environmental Policy, Faculty of Water Sciences, University of Public Service, 2 Ludovika tér, 1083 Budapest, Hungary
2   Max Planck Institute for the Physics of Complex Systems, 38 Nöthnitzer Str., 01187 Dresden, Germany
3   Department of Hydraulic Engineering, Faculty of Water Sciences, University of Public Service, 12 Bajcsy-Zsilinszky u., 6500 Baja, Hungary
4   General Directorate of Water Management, 1/D Márvány u., 1012 Budapest, Hungary
5   Doctoral School of Military Engineering, University of Public Service, 9-11 Hungária krt., 1101 Budapest, Hungary
6   Instituto de Altos Estudos da Paraíba, Rua Silvino Lopes 419-2502, João Pessoa 58039-190, Brazil
*   Correspondence: janosi.imre.miklos@uni-nke.hu
†   All authors contributed equally to this work.

Abstract: In this mini-review, we present evidence from the vast literature that one essential part of the coupled atmosphere–ocean system that makes life on Earth possible, the water cycle, is exhibiting changes along with many attributes of the global climate. Our starting point is the 6th Assessment Report of the IPCC, which appeared in 2021, where the almost monograph-size Chapter 8, with over 1800 references, is devoted entirely to the water cycle. In addition to listing the main observations on the Earth globally, we focus on Europe, particularly on the Carpathian (Pannonian) Basin. We collect plausible explanations of the possible causes behind an observably accelerating and intensifying water cycle. Some authors still suggest that changes in the natural boundary conditions, such as solar irradiance or Earth's orbital parameters, explain the observations. In contrast, most authors attribute such changes to the increasing greenhouse gas concentrations since the industrial revolution. The hypothesis being tested, and which has already yielded convincing affirmative answers, is that the hydrological cycle intensifies due to anthropogenic impacts. The Carpathian Basin, a part of the Danube watershed, including the sub-basin of the Tisza River, is no exception to these changes. The region is experiencing multiple drivers contributing to alterations in the water cycle, including increasing temperatures, shifting precipitation regimes, and various human impacts.

Keywords: global climate change; accelerating hydrological cycle; floods and droughts; groundwater deficit

1. Introduction

On 13 October 2022, the U.S. Geological Survey (USGS) released the newest version of their classical (about twenty years old) water cycle diagram, see Figure 1. For the first time, the new diagram includes anthropogenic contributions such as grazing water use, urban runoff, domestic, municipal, and industrial water use, besides the fundamental components such as evaporation, transpiration, precipitation over land and ocean, and runoff [1]. At the same source, pool volumes (km^3) and flux rates (km^3/year) are available for each item following Abbott et al. [2]. Indeed, without considering the human impacts, one cannot analyze and understand the global water cycle, particularly the changes in the water cycle that we live with.
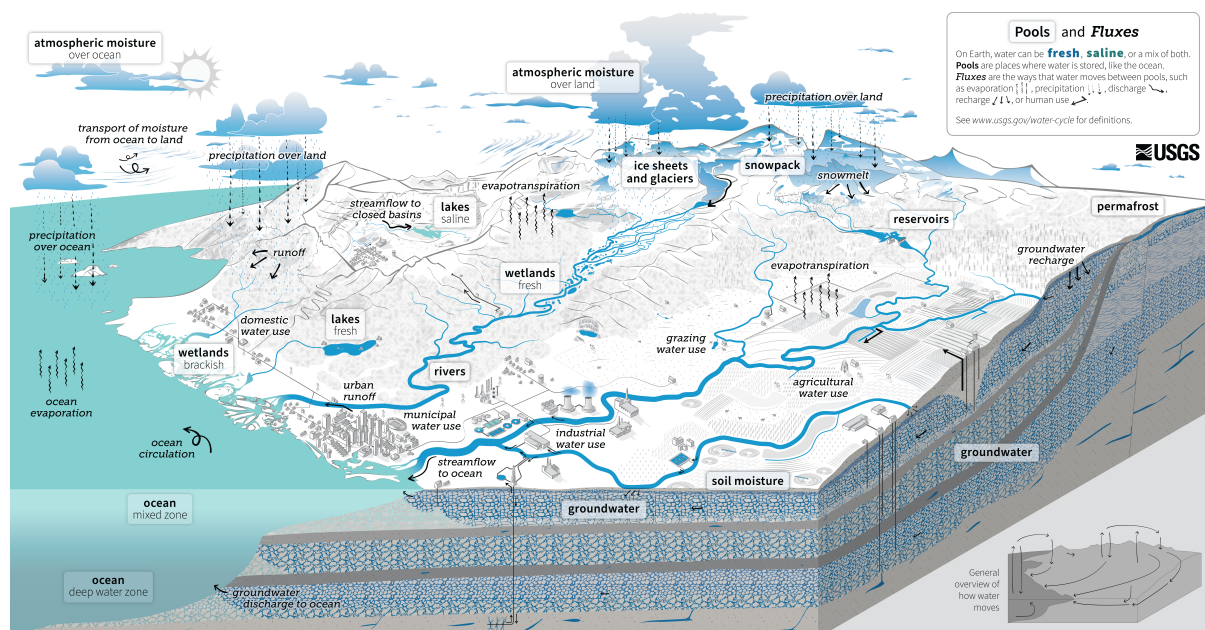
Figure 1. The updated U.S. Geological Survey (USGS) water cycle diagram. (Source: https://www.usgs.gov/media/images/water-cycle-png, last accessed on 14 April 2023, public domain).

The global population explosion during the 20th century (from 1.65 to 6.11 billion) resulted in a six-fold increase in water use and continues to grow by roughly 1% per year since the eighties [3]. The growth is driven by population increase, economic development, and changing consumption patterns, e.g., slowly improving water and sanitation services in developing countries. Despite the continuous development of water-related technologies, up to 80% of the world's population may suffer from water stress or severe water scarcity, albeit often seasonally [2–4]. There are many signs that climate change shifts the water cycle toward an increased seasonal variability, resulting in a more erratic and uncertain water supply. Such changes can enhance problems in already water-stressed areas and induce water stress in locations where it has not been common previously [5–9].

Given the central role of water in human civilization, the successful implementation of almost all Sustainable Development Goals depends on water [10]. Environmental integrity provides the foundation for a reliable water resource base, and a well-managed environment provides essential and low-cost public goods and services. If these aquatic environments and related services are managed with a long-term perspective, they offer a solid foundation for human well-being and economic development. This is the essence of sustainability [10–15].

Chapter 8 of the Sixth Assessment Report (AR6) of the Intergovernmental Panel on Climate Change (IPCC) is devoted to water cycle changes [4]. This (almost monograph-size) chapter cites more than 1800 references, and there are no recent or previous reviews which could be more comprehensive than this. Repeating any part of the chapter apart from the logical framework of problem settings would be unnecessary. In this mini-review, we begin with the conclusions of Douville et al. [4] relevant to regional scales, particularly for the Carpathian Basin. Additionally, since several results have been published in local journals in Hungarian, we survey the related literature missing from the scope of IPCC AR6.

We will argue that the Carpathian Basin is not unique on Earth; the observed local changes are common in many mid-latitude regions. The central hydro-meteorological tendencies are the warming faster than the global average, increasing water-holding capacities in the troposphere, rearrangement of large-scale atmospheric wind systems, changes in the spatial and temporal distribution of rain, diminishing snow, especially from lowland areas, decreasing river discharges, changes in the timing of annual maximum water levels in rivers, generally decreasing groundwater levels, and some other local changes affecting

the shallow lakes. In order to support some conclusions related to water level statistics, we exhibit results for three hydrometric time series along the river Tisza, the longest tributary of the Danube that flows through the Great Hungarian Plain. Since hydrological systems are inherently nonlinear as the whole climate system, thus appropriate methods in data analysis and numerical models should adopt nonlinear approaches.

2. Data and Methods

2.1. Geographic Settings

The Carpathian (Pannonian) Basin is a lowland region in the southeastern part of Central Europe, geographically bounded by the Carpathian Mountains, the Alps, the Dinaric Alps (Dinarides), and the Balkan mountains (see Figure 2). It can be considered a compact catchment area of the middle section of the river Danube (entering through the north-western gap between the Carpathian Mountains and the Alps into the basin). The Danube is the second-largest river in Europe. It flows through ten countries, of which seven have at least some territories in the Carpathian Basin (indicated by italics): Germany, *Austria (AT)*, *Slovakia (SK)*, *Hungary (HU)*, *Croatia (HR)*, *Serbia (RS)*, Bulgaria, *Romania (RO)*, Moldova, and *Ukraine (UA)*. The Danube collects water from 27 larger and over 300 smaller tributaries along its flow track of about 2850 km. The largest tributaries in the Carpathian Basin are the Tisza, Sava, and Drava. For a subregional divison, see e.g., Figure 3 in Ref. [16].
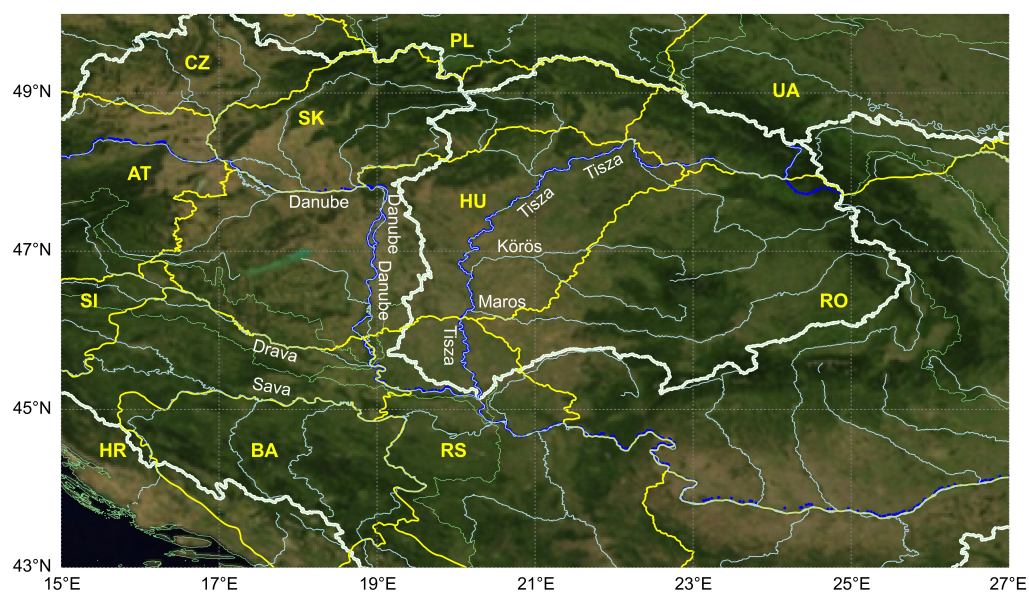

Figure 2. Political borders and country codes (yellow), rivers inside and through the Carpathian Basin (light blue), river center-lines of Danube and river Tisza (blue, where it was available), and the boundaries of sub-basins of the Danube and major tributaries (thin light green). The basin boundaries of the Danube and Tisza are emphasized by white coloring. This map was created using `Python` (3.8.8) and the `Basemap` library (1.3.2), https://matplotlib.org/basemap/. Background satellite photo: NASA Visible Earth project, https://visibleearth.nasa.gov/ (last access: 13 April 2023).

2.2. Data Sources

This mini-review is mainly based on literature data and conclusions; the unique feature is that we survey relevant Hungarian papers of relatively limited access for non-Hungarian-speaking experts. To illustrate some points in this paper, we evaluated 23-year-long water level records of the Tisza River obtained from the General Directorate of Water Management, Budapest, Hungary (https://www.ovf.hu/en/, accessed on 4 May 2023). Instead of a full-scale analysis, here we present representative examples for three hydrometric stations. The river basin data are collected and maintained by the HydroSHEDS project initiated in 2006 by the World Wildlife Fund. Watershed information is available in a series of

shapefiles (https://www.hydrosheds.org/products/hydrobasins, accessed on 4 May 2023), 'level04' data for major tributaries are used in Figure 2 [17].

3. Results

We begin with the list of conclusions of IPCC AR6, Chapter 8 by Douville et al. [4], which are relevant to the Carpathian Basin and other European regions.

- Modifications of Earth's energy budget by anthropogenic activities drive substantial and widespread changes in the global water cycle. There are more and more pieces of evidence that global mean precipitation and evaporation increase with global warming. The increase in global precipitation is determined by a robust response to global mean surface air temperature (likely 2–3% per 1 °C). Land use and land-cover changes also drive regional water cycle changes through their influence on surface water and energy budgets (high confidence).
- Warming over land drives an increase in the atmospheric water holding capacity by around 7% per 1 °C enhancing the severity of droughts (high confidence). More significant warming over land than over the ocean changes large-scale atmospheric circulation patterns and decreases relative humidity in the continental boundary layer, which contributes to regional droughts (high confidence). Parallel to it, increasing water content in the middle and higher troposphere intensifies heavy precipitation events that enhance the severity of flood hazards.
- Land-use change and water extraction for irrigation have influenced local and regional responses in the water cycle since the mid-20th century (high confidence). Extended deforestation has decreased evapotranspiration and increased runoff over the deforested regions. Urbanization has probably increased local precipitation and runoff intensity (high confidence). Groundwater depletion, mainly for irrigation, has occurred since at least the start of the 21st century (high confidence).
- Anthropogenic surface solar radiation modification (primarily by aerosol emission) could drive abrupt changes in the water cycle (high confidence). The modification is spatially heterogeneous (high confidence), and it probably will not fully mitigate the greenhouse-gas-forced water cycle changes (medium confidence) [18].
- Paleoclimatic records indicate that a collapse in the Atlantic Meridional Overturning Circulation (AMOC) triggers abrupt shifts in the water cycle (high confidence), particularly severe droughts in Europe. High-resolution globally coupled numerical models suggest that such dry spells decrease grass and crop productivity over the European land, both in mountainous and lower areas [19,20].

3.1. Primary Drivers of the Water Cycle

It is well understood that Earth's energy balance determines precipitation and evaporation. Water cycle changes on regional scales are expected to be determined by the transport of moisture. In a warming climate, main characteristics such as precipitation intensity, duration, and annual distribution are changing, however, in a complex way. Besides local factors such as evapotranspiration rate, aerosol load, and human use, changes in the large-scale transport processes are equally important [4].

3.1.1. Temperature Trends

It has been known for rather a long time that the European land warms faster than the world average [21–25] (see the data at https://www.eea.europa.eu/ims/global-and-european-temperatures, accessed on 4 May 2023). Meteorological observations in Hungary can be considered representative of the Carpathian Basin because the country's entire territory is in the inner lowland. Accordingly, global warming is significantly observable (around 2 °C in the past 50 years). Clear pieces of evidence are based on analyses of hourly or daily temperatures, [26–28], extreme values [29,30] or the frequency of warm spells [29,31]. The representativity is supported by evaluation of temperature time-series

in Bačka (Serbia) [32] and over the Sava River watershed (Bosnia and Herzegovina) [33], where each meteorological station also recorded very similar warming trends.

The Sun is the external energy source to Earth; solar radiation keeps the elevated temperature necessary for liquid water and life. The total solar irradiance (TSI) measures the total power from the Sun falling on a perpendicular unit area at the top of the atmosphere, in units of Wm^{-2}. TSI is the wavelength integral over the entire spectral range of irradiance. Direct satellite measurements of TSI have been available since 1978. The period of four and a half decades is moderately relevant in the climate change context. Nevertheless, there has been a vivid debate in the literature about the possible natural origin of global warming. Obviously, the variability or trends in TSI was the main target. It is evident that variations in solar activity (thus in TSI) influence weather and climate on every time scale [34,35]. The key question is the decadal or millennial trend; an increasing TSI presumably warms the Earth. A very recent review by Chatzistergos, et al. [36] concludes that the existing (over twenty) long-time reconstructions of TSI time series do not exhibit significant tendencies in the past 200-300 years, and all of them suggest a slightly decreasing trend since 1996.

It is worth noting that TSI is the external boundary condition for the climate system. In a weather or climate context, how much energy is reflected and absorbed in the atmosphere and surface is more relevant. Indeed, while TSI has a weak negative trend, surface solar radiation (SSR) has a positive tendency at least from the middle of the eighties in the Carpathian Basin (about 1%/decade) [37–39]. This tendency is not unique. It is widely accepted that surface solar radiation experienced a pattern of dimming (shorter sunshine durations) from the 1950s to the 1980s, followed by a period of brightening (longer sunshine durations) from the late 1980s to the early 2000s in the United States, Europe, and certain regions in Asia. Previous research has attributed this trend to aerosols (from anthropogenic and volcanic sources) and clouds, the main potential factors contributing to continental dimming and brightening [40,41].

According to the IPCC AR6, the increase in greenhouse gas emissions due to human activities has resulted in a temperature rise of around 1.1 °C since the beginning of the twentieth century [42]. Changes in TSI or SSR alone cannot explain the observations. This evaluation is supported by better observational data that help determine historical warming trends and advancements in scientific knowledge regarding the climate system's response to anthropogenic greenhouse gas emissions.

3.1.2. Changing Wind Regimes

Wind fields play a major role in the large-scale redistribution of vapor and water, and they are the main component of weather systems. As reviewed by Gulev et al. [42] (Chapter 2 in IPCC AR6), the winter zonal wind speeds in the mid-troposphere have strengthened. In contrast, they have weakened over the Northern Hemisphere in summer, although the trends are mostly statistically non-significant (see Figure 2.18 in Ref. [42]). Similarly, the data from ERA5 global reanalysis [43] indicate a slight general weakening tendency of surface wind speeds over the northern part of European land (mainly Scandinavia). However, the trends in most of the geographical locations are not robust (see Figure 2.19 in Ref. [42]). There are periods lasting a couple of years when local trends are alternately increasing and decreasing [44]. As for the Carpathian Basin, reanalysis data indicate statistically significant negative trends in the mean westerly wind speeds at the higher tropospheric levels and positive trends at the very high stratospheric levels [45].

From the perspective of the water cycle, one particular aspect is the firm increase in heat extremes in Europe determined strongly by large-scale atmospheric circulation and jet stream states [23,25,31]. Recently, Rousi et al. [25] found that European heat wave tendencies (particularly the persistent ones over 6 days) can be strongly linked with more persistent double-jets over Eurasia (besides the usual mid-latitude jet around at 40–45° N, a weaker jet builds up at ∼70–75° N).

3.1.3. Atmospheric Moisture

Over land, the main components of total evaporation (interception and transpiration) determine the amount of atmospheric water. The contribution of the fluxes is mostly controlled by vegetation and dominated by transpiration (about 60% of total land-surface evaporation) [46]. Accordingly, atmospheric moisture depends on local circumstances such as vegetation coverage and land use of large spatial variability.

The IPCC AR6 (Chapter 2) reports positive global total column water vapor trends since the eighties of the past century when globally representative combined infrared and microwave satellite observations started, with medium confidence of the trend magnitudes [42]. Globally, the total atmospheric water vapor is increasing by about 1% per decade. Changes are more significant in the upper troposphere, consistent with thermodynamics [47].

Since the 1970s until the turn of the century, specific humidity has increased over most of the continuously monitored parts of Earth. Global mean values exhibited a plateau between 2000–2014, when the increasing trend resumed, particularly over land [42] (also see Figure 1 in [47]). The mean specific humidity over land and the Atlantic Ocean has remained well above the 1973–2019 average (see Figure 2.13b in [42] and Figure 1 in [47]).

The increasing tendencies of specific humidity are significant across most of the land and ocean regions [42,47]. In contrast, trends in relative humidity show distinct spatial patterns with generally increasing trends over the higher latitudes and the tropics and generally decreasing trends over the sub-tropics and mid-latitudes, particularly over land areas (Figure 2.13c in [42], Figure 8 in [47]).

In the Carpathian Basin, global change affects all climate variables [48], including the water-holding capacity of the atmosphere. An increasing trend in the Penman–Monteith reference evapotranspiration on a daily scale was detected in the decades between 1961 and 2010 [49]. The average trend obtained was 0.868 mm/year, resulting in a 42.5 mm mean increase during these five decades. The biggest local changes are close to 125 mm in flat areas in the north-western part of the basin.

The high spatial and temporal variability of atmospheric moisture is nicely demonstrated by Cséplő et al. [50], where 60 years of the climatology of mist and fog has been studied in Hungary. Clear trends were not really observed; instead, the temporal behavior exhibited firm site dependence [50]. However, Ilona et al. [51] collated historical fog records for 1886–1916 with recent data for 1990–2020. While decadal trends were not significant, the mean number of foggy days in a year increased by 16.2 d during the recent three decades compared to the turn of the nineteenth century [51].

3.1.4. Precipitation Trends

In summary, globally averaged land precipitation has increased since the middle of the 20th century; however, such trends were insignificant in the first five to six decades. An enhanced increase in global land precipitation has been observed since the eighties. As is well known, precipitation exhibits substantial temporal and geographical variability as well as regional heterogeneity [42]. Interestingly, Schneider et al. [52] compared land surface precipitation climatologies for a 30-year reference period 1931–1960 with three decades at around the millennium (1981–2010) but could not identify significant trends. This might be caused by the large variabilities, data coverage problems over time, and some technical issues related to the rain-gauge networks [52].

As for the Carpathian Basin, analyses by Bartholy and Pongrácz [30], Bartholy and Pongrácz [53], Bartholy and Pongrácz [54] revealed that in the second half of the 20th century, the intensity and frequency of extreme precipitation events had increased, notably since the eighties, while the total (annual) amount slightly decreased. An earlier study by Domonkos [55] already detected a significant drop of annual precipitation totals in the 20th century based on aggregated monthly data. Ilona et al. [51] also revealed significant changes in the aggregated values of precipitation by comparing historical (1871–1918) and recent (1971–2020) periods. At lowlands, the drop in precipitation totals is larger than 20%

during spring and autumn seasons. A shift in the distributions is observed only at a few stations. Note that significant trends were not really detected either in the historical data or in recent decades; the latter is somewhat surprising [51]. Lakatos et al. [56] analyzed sub-daily precipitation statistics in the region. Some territories are strongly undersampled; nevertheless, significant increasing tendencies of the mean 1-h precipitation intensity are detected mainly in the northern regions during summer and autumn.

In addition to aggregated values and intensities, the temporal distribution of precipitation is crucial for the water cycle context. An earlier analysis of precipitation data for 1891–1990 revealed significant climate fluctuations in the region. A trend of definite aridification was already detected in the 20th century [57,58]. However, two aridity indices (De Martonne Aridity Index and Palmer Drought Severity Index) assessed for data from 78 meteorological stations from 1931–2017 indicated a lack of significant tendencies [59]. Similarly, Spinoni et al. [48] could not identify clear trends (apart from a mild frequency increase), but statistical significance tests were not performed because of the lack of an unambiguous definition of drought. Such results clearly demonstrate that methodologies and other factors (especially finite size effects, inhomogeneities, data scarcity, etc.) have primary importance in climate research because different works often lead to controversial conclusions even when the target is the same. Comprehensive data analysis for Hungarian records in the period of 1901–2013 revealed insignificant trends, apart from detecting the intensification of summer precipitation and an increasing tendency of drought years [29]. Climate cycles and oscillations are also revealed in precipitation time-series in the Carpathian Basin, with a fragile relationship with teleconnections [60].

3.2. Hydrological Trends

Since the severity of very wet and very dry events increases in a warming climate (with significant regional and seasonal inhomogeneities), such changes obviously influence all hydrological variables. Major tendencies are detected in the midlatitudes, particularly in snow-dominated river basins. Increasing temperatures cause reduced winter snowpack, which melts earlier in spring [4,61]. Furthermore, temporal shifts of seasonal minima and maxima of the hydrological regimes are observed mainly in snow and glacier melt-dominated alpine catchments [4,62]. Another recent study based on the European Flood Database [63] found that trends in the once-in-a-century flood in Europe show a similar geographical pattern as trends in mean floods over the period 1960–2010, with some variations depending on the region and the size of the catchment area [61]. Recent floods have been so much more severe than previous events that flood risk estimation methods have significantly changed in the affected regions [64]. A valuable open-access data bank on floods from 1985 is the Dartmouth Flood Observatory (https://floodobservatory.colorado.edu, last access: 27 January 2023), which later moved to the Colorado University. The data bank provides global geographic coverage. Information is collected both from news reports and satellite observations to identify, measure, and map floods [65]. However, there are only four records for Hungary from 1985, probably because inundation areas must be sufficiently large to be detected by satellite observations (and local news is in Hungarian).

3.2.1. River Discharge Rates

Blöschl et al. [66] extracted regional trends of river "flood" discharges in Europe for 1960–2010. The analysis is based on river discharge observations of 3738 hydrometric stations for the period 1960–2010 (the data are available at https://github.com/tuwhydro/europe_floods, last access: 27 January 2023, [63]). The quotation mark is justified because the term "flood" is consistently used in the paper as a proxy for the annual maxima of discharges in each calendar year. Local maximum levels are always present in any record; however, real floods with inundations are exceptional. Statistically significant trends in rare real flood events are difficult to detect because of the limited length of homogeneous time series. The main result is reproduced in Figure 3. The three numbered subregions belong to different primary drivers. 1: Northwestern Europe: Increasing rainfall and

soil moisture. 2: Southern Europe, decreasing precipitation and increasing evaporation. 3: Eastern–Northeastern Europe, decreasing precipitation and earlier snowmelt. According to Blöschl et al. [66], the area of the Carpathian Basin belongs to subregion 2 with a decreasing annual maximum discharge rate tendency of 5–12% per decade. Bertola et al. [67] selected the longest records from the same discharge database [63] (at least 40 years, 2370 hydrometric stations) and analyzed different "flood" quantiles for the subregions numbered in Figure 3. The results in [67] reveal that the trends in northwestern Europe are generally positive. In small catchments (up to 100 km^2), the 100-year flood increases more than the median value. Contrarily, in medium and large catchments, positive trends fade, and even negative tendencies appear. In southern Europe, flood trends are generally negative and do not depend on the return period. The catchment area is essential again; the larger the catchment, the more negative the tendency. Unfortunately, the database [63] contains only a limited number of records for the Carpathian Basin; thus, studies of selected records cannot precisely describe local changes in river discharges.

In a detailed statistical analysis, Rottler et al. [61] assessed trends of river discharge rate data in a few central European catchments for the period 1869–2016. Four gauging stations provided the exceptionally long time series for the rivers Inn and Rhine. The authors detected significant changes in the seasonality of river runoff for rainfall and snowmelt-dominated locations, mainly in the second half of the twentieth century. The seasonality of river runoff decreased during the past decades due to the atmospheric warming tendency since a growing fraction of total precipitation became liquid. An important observation of the authors is that even robust linear fits to the data either do not indicate or strongly underestimate tendencies, while a nonlinear procedure clearly reveals regime shifts [61].

Berghuijs et al. [68] evaluated flood synchrony scales defined by the mean distance over which two or more rivers peak near synchronously. The same data bank [63] was used as in Refs. [61,66,67]. Flood synchrony scales can be much larger than the extent of individual catchments, with large (more than one order of magnitude) regional variations. Flood synchrony scales have increased by around 50% during 1960–2010, and they are serially correlated, meaning that spatially extensive flood years tend to cluster [68]. Kemter et al. [69] used the same methodology (flood synchrony scales) for the same data bank [63] and revealed strong positive correlations between flood magnitudes and spatial extents for 95% of the stations.

Local studies [70–73] revealed that higher peak discharges were observed in the Danube between 1941 and 2005 compared to the period 1876–1940. In late March, the runoff excess values were nearly 500 m^3/s. Almost the same peak drops were detected in late summer and early autumn: around 550 m^3/s [70]. The spring rising tendency can be explained by the earlier melting of the snow, which is the consequence of increasing air temperature. Summer discharge drops can be attributed to elevated evaporation and the earlier supply withdrawal from snow melt. Similar tendencies were reported for two tributaries, the rivers Drava and Mura, during the period 1960–2019 [73]. There is no wonder that the number of dike failures in the Carpathian Basin has sharp maxima at the peak discharges during spring [74,75]. Notably, rain on top of snow often triggers extreme river runoffs [76,77]. Half of the extreme floods with extensive inundations along the river Danube was recorded since the beginning of the 20th century during the past three to four decades [78].
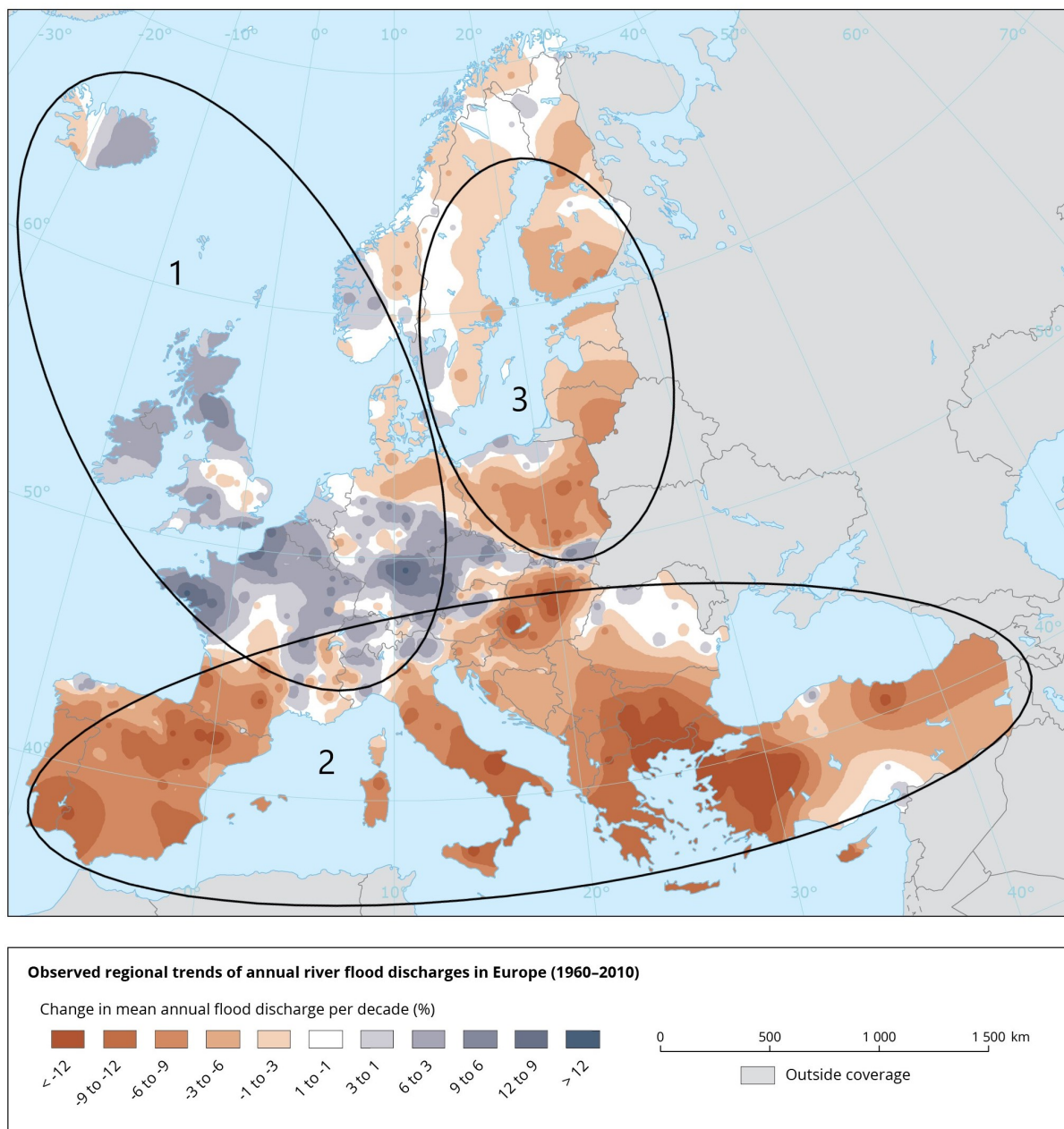
Observed regional trends of annual river flood discharges in Europe (1960–2010)

Change in mean annual flood discharge per decade (%)

< -12 | -9 to -12 | -6 to -9 | -3 to -6 | -1 to -3 | 1 to -1 | 3 to 1 | 6 to 3 | 9 to 6 | 12 to 9 | > 12

0   500   1 000   1 500 km

Outside coverage

Figure 3. The map illustrates the geographic distribution of linear trends in the annual maximum of daily river discharge for the period 1960–2010 (data from 2370 hydrometric stations). Blue/red denotes increasing/decreasing "flood" discharges in units of % change of the mean annual maximum discharge per decade. Numbered subregions belong to different primary drivers; see the text. (Source: European Environment Agency (EEA), https://www.eea.europa.eu/data-and-maps/figures/observed-regional-trends-of-annual, last accessed 14 April 2023, with permission, originally published in Ref. [66]).

3.2.2. Timing of Extreme Water Levels

Blöschl et al. [62] and Hall and Blöschl [79] reported that climate change has also affected the timing of annual maximum water levels over continental Europe in the period 1960–2010. The decadal trend map in [62] is somewhat spotty, with smaller and larger areas of consistent shifts to later or earlier annual maxima alternating next to each other. The northern part of the Carpathian Basin exhibits 4–14 days shifts to later peak river discharges, while an opposite tendency dominates in the south. As mentioned before, data scarcity does not permit an adequate explanation in the region, mainly because the closed

basin exhibits different tendencies in the northern and southern parts. The Irish Island is also rather tiled, suggesting that whatever causes high water levels is strongly local and probably the consequence of several factors.

In order to compare the results of [62] with local observations, we evaluated water level records of 22 hydrometric stations along the river Tisza. Tisza is the largest tributary of the main regional river Danube; its catchment area is around 156,000 km^2 [80]. The time series are rather strongly correlated; therefore, we illustrate data for three representative stations here. One is situated in the upper Tisza (Záhony), and two of them are in the middle river section (Tiszapalkonya and Csongrád, see Figure 4). The temporal sampling is rather hectic at almost all stations changing randomly between 15 min and 27 h; see Figure 5. Fortunately, longer gaps are not present; therefore, it is improbable that essential events such as floods are missed.
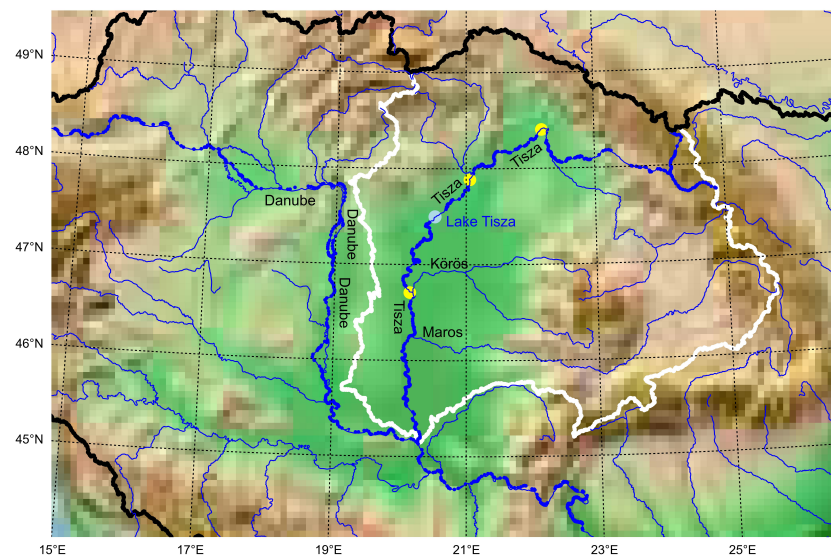

Figure 4. Map of major rivers (major tributaries in Hungary are annotated) and the three representative measuring stations along river Tisza (yellow): Záhony (48.40° N, 22.18° E), Tiszapalkonya (47.88° N, 21.06° E) and Csongrád (46.71° N, 20.14° E), from north to south. The basins of Tisza (white) and Danube (black) are delimited. The hydrometric stations are also identified in the next figures. This map was created using `Python` (3.8.8) and the `Basemap` library (1.3.2), https://matplotlib.org/basemap/ (last access: 13 April 2023).
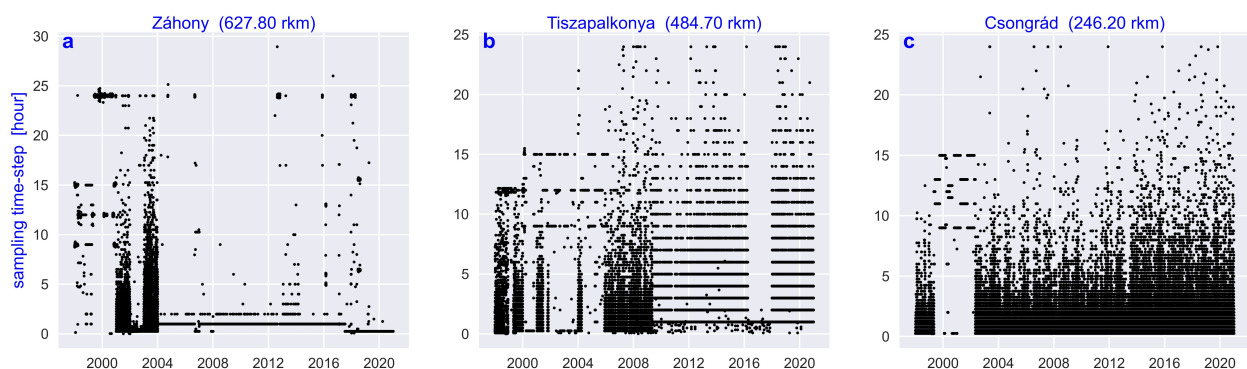

Figure 5. Sampling interval (in units of hours) as a function of calendar date and time (covering 23 years) for the three hydrometric stations (see the titles of panels). In the records, timestamps are given, thus the `Python` routine `matplotlib.pyplot.plot_date()` correctly places data along the horizontal time axis independently of timestep size. The stations are indicated in the title lines with the locations (measured in river km from the Danube–Tisza confluence) and in Figure 4 by yellow symbols.

Figure 6 shows the time series for the representative stations. The strong correlation among the curves is apparent. At first, a clear annual periodicity is not easy to resolve. We performed frequency analyses using the Lomb–Scargle Periodogram method [81,82] created exactly to handle unevenly sampled time series. A naive use of Fourier transform indeed fails for such data. The significant peaks are around one year (Záhony: 367.7 d, Tiszapalkonya: 365.9 d, Csongrád: 364.7 d), and slower oscillatory modes are weaker and not consistent for the time series. However, annual maxima are always present, even when mean water levels are extremely low throughout a given year (e.g., see the years 2003, 2014, and 2015 for all stations). The occurrences of annual maxima far exceed the number of real floods with inundations along the river bed.

We determined the day of year for the dates of annual maxima and minima of time series, Figure 7 illustrates the results for the three stations. Linear fits were performed using the same Theil–Sen robust linear estimator (`Python` library `SciPy`, routine `scipy.stats.mstats.theilslopes()` [83]) as carried out by Blöschl et al. [62]. The occurrences of both extreme values are distributed widely in the calendar, but the overall linear tendencies for the maxima are roughly in agreement with the coloring of Figure 1 in [62]. Annual peak water levels shift to later dates more or less systematically. Actual flood events with inundations (denoted by stars in Figure 7) rarely happened during the 23 years (three events at Záhony, five at Tiszapalkonya, and four at Csongrád) and, therefore, a trend analysis is not feasible, as expected. Annual minimum water levels (red in Figure 7) exhibit much weaker tendencies, if any. Their timing is more consistent than for maxima, particularly at higher river sections. The large scatter in the calendar suggests that no single mechanism triggers extreme water levels; snow melt, rain-on-snow events, evaporation, infiltration, pluvial flows, river bed erosion, groundwater levels, and others might contribute). Certainly, further studies are required to shed light on the background.
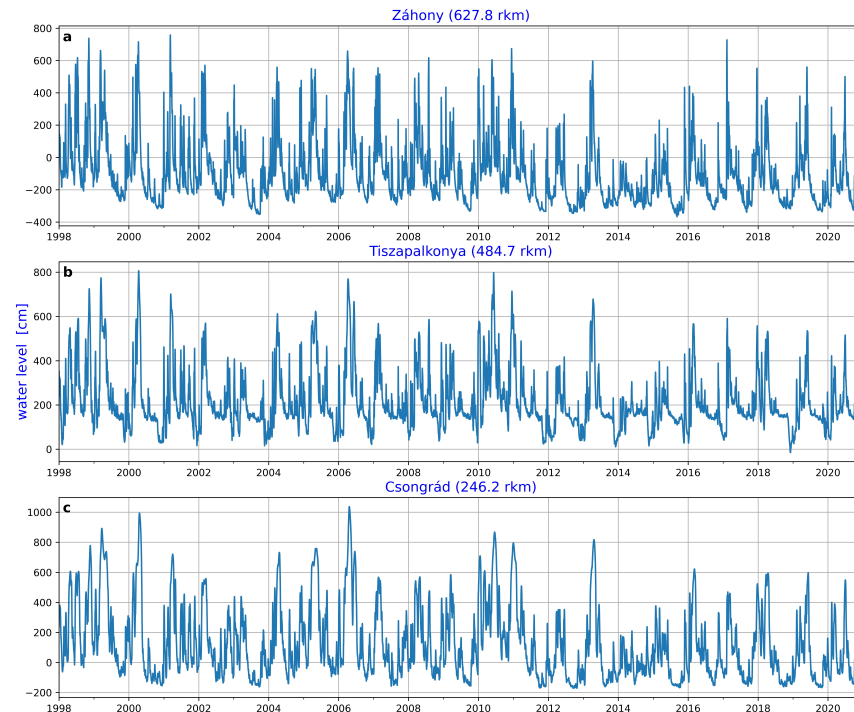

Figure 6. Time series of water levels for 23 years with hectic uneven temporal sampling between 15 min and 27 h. In the records, timestamps are given, thus the `Python` routine `matplotlib.pyplot.plot_date()` correctly places data along the horizontal time axis independently of timestep size. The stations are indicated in the title lines with the locations (measured in river km from the Danube–Tisza confluence) and in Figure 4 by yellow symbols. As usual, water levels are not absolute values but relative to the zero point of the local gauge.
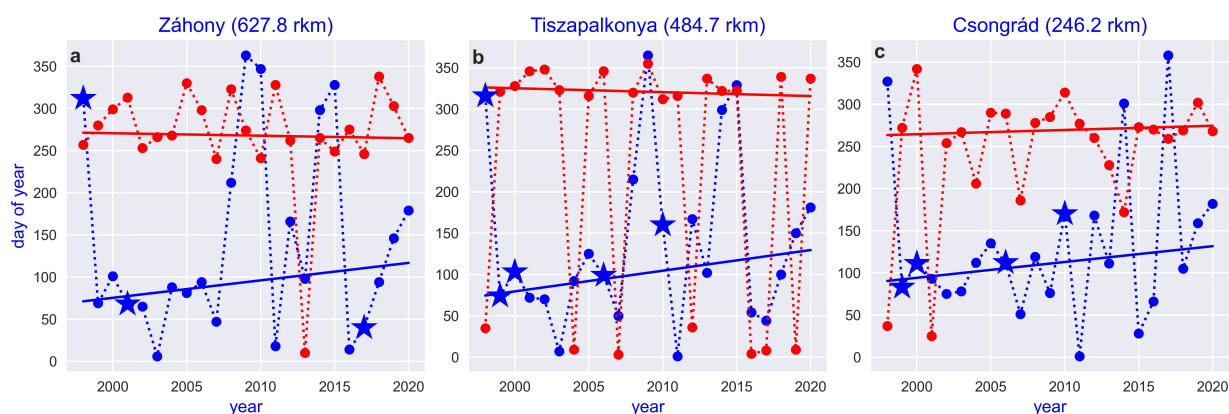
Figure 7. Day of year of the annual maximum (blue) and minimum (red) water levels at the three representative measuring stations along the river Tisza (see title lines). Linear fits (straight lines) are obtained by the Theil–Sen robust linear estimator, see text. Stars indicate real flood events (data from the General Directorate of Water Management).

3.2.3. Groundwater Issues

Despite the importance of groundwater as the largest part of blue water [84], its volume is probably the least-known storage pool in the hydrosphere [85]. Besides the challenges to estimating the pool volume deep underground, the maximum depth of groundwater reserves is loosely defined; the usual limit being around 4 km [2,85,86]. Notably, huge quantities of hot saline water (full also with dissolved minerals) were found even at depths below 12 km (Kola Peninsula, Superdeep Borehole) [86]. The global volume of renewable/non-renewable groundwater reserves is estimated in rather wide ranges: 0.3–1.2/8–23 (million km^3) [2,87]. Similarly, uncertain estimates are available for groundwater recharge fluxes. Saline groundwater recharge is supposed to be 13,000 ± 60% km^3/year, while the freshwater recharge flux globally is around 250 ± 90% (!) km^3/year [4].

Groundwater resources in the Euro-Mediterranean countries (including most of Europe, North Africa, and the Arabian Peninsula, see Figure 1 in [88]) supply a large part of the population's water demand and are influenced by human utilization and climate impacts. Significant groundwater table declines have already been observed in numerous geographic locations, indicating a growing imbalance between groundwater extraction and natural recharge. Analyses of the mean annual trends reveal significant decreases in groundwater resources in many countries of Europe, Northern Africa, and the entire Arabian Peninsula (in about 70% of the studied region) [88–90]. The spatial mean of the trends across the Euro-Mediterranean region is −2.1 mm/year, with the most substantial declines observed in Iraq and Syria (−8.8 and −6.0 mm/year). Moreover, countries in central and eastern Europe are affected considerably (the mean value over Hungary is around −5.7 mm/year) [88]. The results clearly indicate growing groundwater stress in the Euro-Mediterranean region, which is expected to grow further.

Shallow lowland groundwater reservoirs in the Carpathian Basin are mostly dedicated for agricultural purposes; thus, a network of wells has already been constructed from the 1930s. A total of 1500–1700 wells (from a recent total of over 1 million) have been working permanently since then serving as a useful source for spatiotemporal evaluation [91–95]. The long time series of groundwater levels exhibit significant variabilities, seasonality, and decadal tendencies [94]. Mainly since the 1970s, a systematic depletion has been characteristic at the majority of observing wells [91,93,95,96]. In the upper aquifers of the Great Hungarian Plain, the annual average groundwater levels have dropped as much as 6–8 m in the period 1970–2010 [92]. A recent estimate over several local catchments (5–10 thousand km^2 each) revealed that the groundwater resources exhibit 3–5 km^3/year changes in both positive and negative directions because of climatic effects. This annual

range is comparable with the human water uses (the total of them in Hungary is around 5 km^3/year); thus, climate change dominates the variations of regional water resources [97].

The exploration of surface water and groundwater interactions has been a key issue in hydrology for a long time (see, e.g., [98] and references therein), especially along rivers. One general direction of the exchange of water masses is when surface water recharges groundwater, while in drought periods, when the surface-water level drops below the groundwater table, the flow direction is reversed. Appropriate mathematical models to solve practical problems of subsurface hydrology are complicated and demand many model parameters [99], particularly in strongly heterogeneous soils [100]. Anthropogenic activities such as damming may drastically change rivers' natural sedimentological and geomorphological conditions. An increasing sediment deposition upstream of hydropower plants results in river-bed clogging and alters the sediment's composition, directly affecting the groundwater's recharge. Possible environmental consequences such as drops in groundwater levels commonly happen and are expected to continue in a warming and drying climate.

River bed erosion, particularly downstream behind dams, is continuously strengthening [101]. Results for the main river Danube in the region show that erosion processes started already at the beginning of the 20th century [102–105]. However, the tributaries Tisza, Drava, Mura, etc., also exhibit similar changes [73,106]. In the past years, bathymetry became the best practice widely to trace river bed changes (often with various equipments installed on drones or even on satellites [107,108]). Besides damming, major drivers of river-bed erosion are river regulation activities, industrial dredging [109,110], and a decrease in natural sediment recharge. The deepening of the river bed has unfavorable effects on the natural environment: lowering of groundwater tables, restrictions of shipping, ecological disturbances, etc., are commonly observed consequences.

3.2.4. Lakes and Climate Change

We mention very briefly lakes in the region for a few reasons. The characteristic forms of still surface water in the Carpathian Basin are shallow lakes (and small swamps), particularly in lowland areas [111]. Tiny lakes and fish ponds contribute weakly to the water cycle.

The largest water body in Eastern–Central Europe is Lake Balaton (average water depth: 3.36 m, mean length: 76.3 km, mean width: 7.95 km, catchment area: 5774.5 km^2, mean volume: 2 million m^3). Water levels are reconstructed back to 2600 years, mostly by sediment analysis. However, the natural variability has been broken since the seventies because the water level of Balaton is actively regulated by the Siófok drainage sluice (the maximum permitted value is 120 cm on the Siófok gauge, and there is no minimum). Because of the growing population around the lake, recent data cannot be easily decomposed for natural processes and human impact. Climate change decreases the recharge through the main inflow river Zala and increases the evaporation rate during the warming summer seasons. However, the water level regulation and other human influences (water extraction into fish ponds, changing land use, restoration of wetlands, etc.) contribute strongly to the water level fluctuations [112–114]. Climate effects are better detectable during the hot summer periods of extremely low water levels when water withdrawal is restricted.

Drying up or huge water deficits of shallow lakes occasionally occur, which is common with the second and third largest shallow Lake Fertő and Lake Velence [115,116]. For example, historical sources report complete dryings up of Lake Fertő in 1693, between 1738–1742, in 1773, and 1811–1813, with the last recorded of such events being between 1864–1870 [117]. The last total drying up of Lake Velence happened in 1864 [115]. Several shallow lakes and surrounding populations experience dramatic changes due to lake and watershed mismanagement and climate change. Eutrophication is a common problem of all shallow lakes, although with substantial variability. As mentioned in the previous paragraph, most shallow lakes have water level problems. Low water levels and shrunk surface areas always result in the deterioration of water quality and loss of aqueous habitat. In a few cases,

water conveyance from other watersheds can improve water balance, but this is a restricted option in the Carpathian Basin. Water quality restoration includes restricting agricultural activities, sewage treatment, dredging, and so on [115].

The most endangered regional still waters are the oxbow lakes along the rivers [118]. They play a unique role in recreational activities; several are important islands for ecosystem conservation. Not infrequently, water is withdrawn from such oxbow lakes for irrigation; sometimes, they were even considered sewage depositories. In Hungary alone, the number of oxbow lakes larger than 4 hectares is 237 [119]. The major problem is that several of them are continuously silting in the lack of sufficient water supply (with a rate of up to 1–3 cm/year); thus, they will disappear soon without intervention [120].

3.2.5. Nonlinearities

Empirical frequency distributions are commonly used to analyze and describe the distribution of data across various fields. In hydrology, rivers are often studied by analyzing their water level changes over time, providing insights into the patterns and trends of the river's behavior.

Figure 8 exhibits the empirical frequency distributions of water level changes for the records of the three hydrometric stations exploited above. Here the strongly uneven sampling steps lead to biased statistics; therefore, a naively drawn histogram from raw data is fully misleading. We used interpolation and downsampling (in periods of sampling steps of 15 min) to produce homogeneous series with a temporal resolution of 12 h (interpolation and resampling was performed by routines in the `SciPy` library in `Python` [83]). The shapes in Figure 8 are far from being Gaussians. Nevertheless, established practice is to provide arithmetic mean values and standard deviations in various tables, while both moments are inherently related to uncorrelated Gaussian noise.
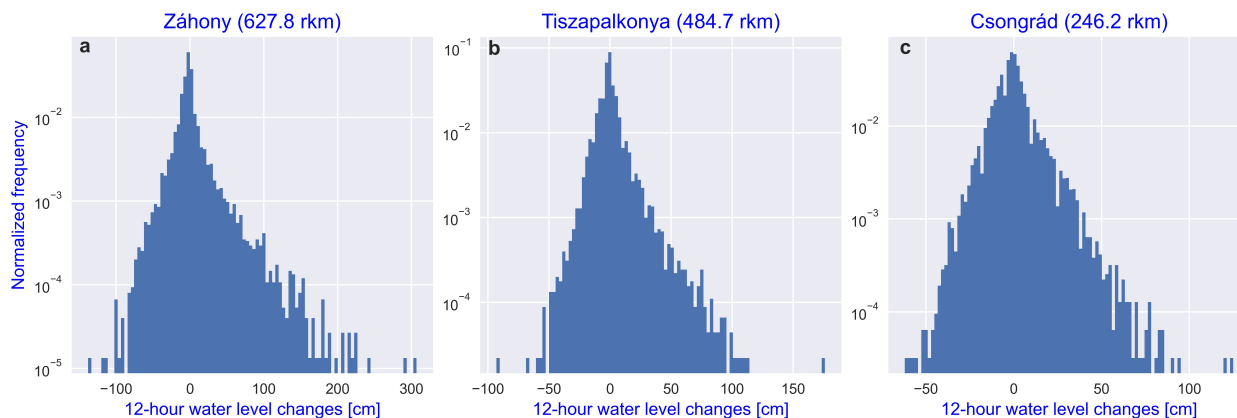

Figure 8. Normalized frequency distribution of interpolated half-day changes in water levels at the three representative measuring stations along the river Tisza (see title lines). The vertical scales are logarithmic.

We emphasize that water level fluctuations are not stochastic (apart from a small-amplitude noise); a river discharge curve is almost deterministic. This means their behavior can be modeled using mathematical equations [121–123]. A slow increase followed by a fast jump is common after heavy precipitation events in the basin or sub-basin; this is characterized by the positive right side of the histograms in Figure 8. An inflection point, which is the point of maximum curvature on the falling limb of the river's hydrograph, marks the point when the river's flow changes from predominantly surface runoff to baseflow.

4. Discussion

As mentioned before, we have dealt intentionally with observations and trends and skipped climate and hydrological projections using numerical models. On regional scales,

simulations suffer from more uncertainties than on global scales. Several problems have been detected at optimal domain selection, lateral boundary conditions (relaxation from buffer zones), initial conditions, physics schemes, or validations of the models [124–127]. As for hydrological modeling and projections, the relative role of parameter uncertainty is even more severe, particularly for catchments with significant changes in flood seasonality. This indicates the lack of robustness in hydrological model parameterization for simulations, especially under transient hydrometeorological conditions [128].

Similarly, green water used exclusively by plants and the soil ecosystem was not in our focus. The hydrological characteristics of soils (e.g., water retention, hydraulic conductivity) are determined by several factors: shape and stability, porosity and bulk density, pore-size distribution, adsorption, water, heat and mass transport processes, biological activity, nutrient supply, etc., and all these are interrelated [129]. Soil water content depends on the groundwater table, mass exchange with nearby water bodies, meteorological circumstances (temperature, precipitation, evapotranspiration, etc.) and frequently changing land use.

Nevertheless, there is no reason to expect a break or reversal of observed trends. The global human population grows, the exploitation of resources increases even faster, the destruction of the global ecosystem and the decrease in diversity is continuous, the environmental pollution accelerates, the concentration of greenhouse gases in the atmosphere continuously rises, and so on. The expected effects of climate change in the midlatitude water cycle can be summarized as follows (valid for numerous regions in all continents):

- Global warming over land continues unabated; shorter winters with diminishing snow and longer summers with frequent and long-continued drought imply decreasing runoffs [4,42].
- The recharge rate into still water bodies and infiltration into the ground decreases; thus, water levels of lakes and groundwater tables are expected to decrease [85,88].
- Changes in the temporal distribution of precipitation trigger more extreme rainfall events during shorter periods, resulting in much larger variability of hydrological parameters and an increasing number of flash floods [130].
- In the Carpathian Basin, floods are expected to occur more frequently in the winter-early spring periods since almost all tributaries of the Danube originate from the surrounding mountains, where the winter becomes warmer and rainy instead of snowy (see Section 3.2, and [131]).
- The same experienced and expected further winter warming decreases the risk of ice-jam floods in the region [132–134].

Water cycle responses are explained by the interaction of multiple drivers, feedback, and time scales. The climate system is inherently nonlinear, such as responses to regional runoff, such as groundwater recharge or water scarcity; simple pattern-scaling techniques do not work. The literature is full of figures where simple linear functions fit evidently nonlinear data sets; even some running operative models widely use assumptions of linear couplings. Rottler et al. [61] demonstrated that linear fits do not detect tendencies in long river discharge time series (despite the fact that the robust Theil–Sen estimator was used), while a nonlinear method (empirical mode decomposition) clearly indicated tendencies appearing in the second half of the past century.

The Carpathian Basin is a region that is particularly vulnerable to the changing water cycle in a warming climate. Droughts are becoming more frequent and severe, with impacts on agriculture, crop yields, ecosystems, and human communities. At the same time, more intense precipitation events are causing flash floods in some areas, further exacerbating the water management challenges faced by the region. The precipitation regime shift also affects rivers and groundwater resources, changing flow patterns and water quality. To address these challenges, measures such as improving water use efficiency, increasing water storage capacity, and enhancing the resilience of ecosystems must be managed.

Author Contributions: Conceptualization, I.M.J., T.B. and A.S.-N.; methodology, I.M.J., B.O.L. and A.S.-N.; software, I.M.J.; formal analysis, I.M.J., T.B., B.O.L., J.A.C.G. and A.S.-N.; investigation,

Data Availability Statement: Water level records are available upon request from the General Directorate of Water Management, Budapest, Hungary (https://www.ovf.hu/en/, accessed on 4 May 2023).

Conflicts of Interest: The authors declare no conflict of interest.

References

1. Duncombe, J. *Not Your Childhood Water Cycle*; Eos: New York City, NY, USA, 2022; Volume 103. [CrossRef]
2. Abbott, B.W.; Bishop, K.; Zarnetske, J.P.; Minaudo, C.; Chapin, F.S.; Krause, S.; Hannah, D.M.; Conner, L.; Ellison, D.; Godsey, S.E.; et al. Human domination of the global water cycle absent from depictions and perceptions. *Nat. Geosci.* **2019**, *12*, 533–540. [CrossRef]
3. UNESCO World Water Assessment Programme. *The United Nations World Water Development Report 2021: Valuing Water*; UN Educational, Scientific and Cultural Organization: Paris, France, 2021. Available online: https://unesdoc.unesco.org/ark:/48223 (accessed on 4 May 2023).
4. Douville, H.; Raghavan, K.; Renwick, J.; Allan, R.; Arias, P.; Barlow, M.; Cerezo-Mota, R.; Cherchi, A.; Gan, T.; Gergis, J.; et al. Water Cycle Changes. In *Climate Change 2021: The Physical Science Basis. Contribution of Working Group I to the Sixth Assessment Report of the Intergovernmental Panel on Climate Change*; Masson-Delmotte, V., Zhai, P., Pirani, A., Connors, S., Péan, C., Berger, S., Caud, N., Chen, Y., Goldfarb, L., Gomis, M., et al., Eds.; Cambridge University Press: Cambridge, UK; New York, NY, USA, 2021; pp. 1055–1210. [CrossRef]
5. Szöllősi-Nagy, A. Life changer in development—Part 2: World's water management faces a turning point (in Hungarian). *Hidrológiai Közlöny (Hung. J. Hydrol.)* **2018**, *98*, 9–16. Available online: https://library.hungaricana.hu/hu/view/HidrologiaiKozlony_2018/?pg=260&layout=s (accessed on 4 May 2023).
6. Gleeson, T.; Wang-Erlandsson, L.; Zipper, S.C.; Porkka, M.; Jaramillo, F.; Gerten, D.; Fetzer, I.; Cornell, S.E.; Piemontese, L.; Gordon, L.J.; et al. The water planetary boundary: Interrogation and revision. *One Earth* **2020**, *2*, 223–234. [CrossRef]
7. Kirovné Rácz, R.M. Climate adaptation in terms of water security in the Danube Countries. *Acad. Appl. Res. Mil. Public Manag. Sci.* **2022**, *20*, 21–36. [CrossRef]
8. Balatonyi, L.; Ligetvári, K.; Tóth, L.; Berger, Á. Water resources management and its homeland security aspect in Hungary. *Sci. Secur.* **2022**, *2*, 519–528. [CrossRef]
9. Szöllősi-Nagy, A. On climate change, hydrological extremes and water security in a globalized world. *Sci. Secur.* **2022**, *2*, 504–509. [CrossRef]
10. Vörösmarty, C.J.; Rodríguez Osuna, V.; Cak, A.D.; Bhaduri, A.; Bunn, S.E.; Corsi, F.; Gastelumendi, J.; Green, P.; Harrison, I.; Lawford, R.; et al. Ecosystem-based water security and the Sustainable Development Goals (SDGs). *Ecohydrol. Hydrobiol.* **2018**, *18*, 317–333. SI: Ecohydrology for the Circular Economy and Nature-Based Solutions towards mitigation/adaptation to Climate Change. [CrossRef]
11. Jaramillo, F.; Desormeaux, A.; Hedlund, J.; Jawitz, J.W.; Clerici, N.; Piemontese, L.; Rodríguez-Rodriguez, J.A.; Anaya, J.A.; Blanco-Libreros, J.F.; Borja, S.; et al. Priorities and interactions of Sustainable Development Goals (SDGs) with focus on wetlands. *Water* **2019**, *11*, 619. [CrossRef]
12. Mulligan, M.; van Soesbergen, A.; Hole, D.G.; Brooks, T.M.; Burke, S.; Hutton, J. Mapping nature's contribution to SDG 6 and implications for other SDGs at policy relevant scales. *Remote Sens. Environ.* **2020**, *239*, 111671. [CrossRef]
13. Mishra, B.K.; Kumar, P.; Saraswat, C.; Chakraborty, S.; Gautam, A. Water security in a changing environment: Concept, challenges and solutions. *Water* **2021**, *13*, 490. [CrossRef]
14. Shaikh, M.A.; Hadjikakou, M.; Bryan, B.A. Shared responsibility for global water stress from agri-food production and consumption and opportunities for mitigation. *J. Clean. Prod.* **2022**, *379*, 134628. [CrossRef]
15. Kang, S.; Kroeger, T.; Shemie, D.; Echavarria, M.; Montalvo, T.; Bremer, L.L.; Bennett, G.; Barreto, S.R.; Bracale, H.; Calero, C.; et al. Investing in nature-based solutions: Cost profiles of collective-action watershed investment programs. *Ecosyst. Serv.* **2023**, *59*, 101507. [CrossRef]
16. Bartholy, J.; Pongrácz, R.; Molnár, Z. Classification and analysis of past climate information based on historical documentary sources for the Carpathian basin. *Int. J. Climatol.* **2004**, *24*, 1759–1776. [CrossRef]
17. Lehner, B.; Grill, G. Global river hydrography and network routing: Baseline data and new approaches to study the world's large river systems. *Hydrol. Process.* **2013**, *27*, 2171–2186. [CrossRef]

18. Turnock, S.T.; Spracklen, D.V.; Carslaw, K.S.; Mann, G.W.; Woodhouse, M.T.; Forster, P.M.; Haywood, J.; Johnson, C.E.; Dalvi, M.; Bellouin, N.; et al. Modelled and observed changes in aerosols and surface solar radiation over Europe between 1960 and 2009. *Atmos. Chem. Phys.* **2015**, *15*, 9477–9500. [CrossRef]

19. Trnka, M.; Rötter, R.P.; Ruiz-Ramos, M.; Kersebaum, K.C.; Olesen, J.E.; Žalud, Z.; Semenov, M.A. Adverse weather conditions for European wheat production will become more frequent with climate change. *Nat. Clim. Chang.* **2014**, *4*, 637–643. [CrossRef]

20. Jackson, L.; Kahana, R.; Graham, T.; Ringer, M.A.; Woollings, T.; Mecking, J.V.; Wood, R.A. Global and European climate impacts of a slowdown of the AMOC in a high resolution GCM. *Clim. Dyn.* **2015**, *45*, 3299–3316. [CrossRef]

21. Klein Tank, A.M.G.; Wijngaard, J.B.; Können, G.P.; Böhm, R.; Demarée, G.; Gocheva, A.; Mileta, M.; Pashiardis, S.; Hejkrlik, L.; Kern-Hansen, C.; et al. Daily dataset of 20th-century surface air temperature and precipitation series for the European Climate Assessment. *Int. J. Climatol.* **2002**, *22*, 1441–1453. [CrossRef]

22. Menne, M.J.; Durre, I.; Vose, R.S.; Gleason, B.E.; Houston, T.G. An overview of the Global Historical Climatology Network - Daily Database. *J. Atmos. Ocean. Technol.* **2012**, *29*, 897–910. [CrossRef]

23. Lorenz, R.; Stalhandske, Z.; Fischer, E.M. Detection of a climate change signal in extreme heat, heat stress, and cold in Europe from observations. *Geophys. Res. Lett.* **2019**, *46*, 8363–8374. [CrossRef]

24. Naumann, G.; Cammalleri, C.; Mentaschi, L.; Feyen, L. Increased economic drought impacts in Europe with anthropogenic warming. *Nat. Clim. Chang.* **2021**, *11*, 485–491. [CrossRef]

25. Rousi, E.; Kornhuber, K.; Beobide-Arsuaga, G.; Luo, F.; Coumou, D. Accelerated western European heatwave trends linked to more-persistent double jets over Eurasia. *Nat. Commun.* **2022**, *13*, 3851. [CrossRef] [PubMed]

26. Lakatos, M.; Bihari, Z.; Izsák, B.; Szentes, O. Global trends and climate change in Hungary in 2020 (in Hungarian). *Sci. Secur.* **2021**, *2*, 164–171. [CrossRef]

27. Lakatos, M.; Bihari, Z.; Izsák, B.; Marton, A.; Szentes, O. Observed climate change in Hungary (in Hungarian). *Légkör (Atmosphere)* **2021**, *66*, 5–11. Available online: https://www.met.hu/downloads.php?fn=/metadmin/newspaper/2022/04/056abbc1a940 abd89a3e61da1de4c5cd-legkor-2021-3.pdf (accessed on 4 May 2023).

28. Barna, Z.; Izsák, B.; Pieczka, I. Trend analysis: Country-wise temperature trend of hourly values (in Hungarian). *Légkör (Atmosphere)* **2022**, *67*, 122–129. [CrossRef]

29. Lakatos, M.; Bihari, Z.; Szentimrey, T. Signs of climate change in Hungary (in Hungarian). *Légkör (Atmosphere)* **2014**, *59*, 158–163. Available online: https://www.met.hu/ismeret-tar/kiadvanyok/legkor/index.php?id=436 (accessed on 4 May 2023).

30. Bartholy, J.; Pongrácz, R. Regional analysis of extreme temperature and precipitation indices for the Carpathian Basin from 1946 to 2001. *Glob. Planet. Chang.* **2007**, *57*, 83–95. [CrossRef]

31. Bokros, K.; Lakatos, M. Analysis of hot spells in Hungary from the early 20th century to the present (in Hungarian). *Légkör (Atmosphere)* **2022**, *67*, 130–140. [CrossRef]

32. Milentijević, N.; Valjarević, A.; Bačević, N.R.; Ristić, D.; Kalkan, K.; Cimbaljević, M.; Dragojlović, J.; Savić, S.; Pantelić, M. Assessment of observed and projected climate changes in Bačka (Serbia) using trend analysis and climate modeling. *Időjárás (Q. J. Hung. Meteorol. Serv.)* **2022**, *126*, 47–68. [CrossRef]

33. Gnjato, S.; Popov, T.; Adžić, D.; Ivanišević, M.; Trbić, G.; Bajić, D. Influence of climate change on river discharges over the Sava River watershed in Bosnia and Herzegovina. *Időjárás (Q. J. Hung. Meteorol. Serv.)* **2021**, *125*, 449–462. [CrossRef]

34. Solanki, S.K.; Krivova, N.A.; Haigh, J.D. Solar irradiance variability and climate. *Annu. Rev. Astron. Astrophys.* **2013**, *51*, 311–351. [CrossRef]

35. Krivova, N.A. Solar irradiance variability and Earth's climate. In *Climate Changes in the Holocene*; Chiotis, E., Ed.; Taylor & Francis, CRC Press: Boca Raton, FL, USA, 2018; pp. 107–119. [CrossRef]

36. Chatzistergos, T.; Krivova, N.A.; Yeo, K.L. Long-term changes in solar activity and irradiance. *arXiv* **2023**. [CrossRef]

37. Kocsis, T.; Jakus, P.; Szabó, B. Analysis of the sunshine duration data between 1968 and 1999 at Keszthelyt (in Hungarian). *Légkör (Atmosphere)* **2012**, *57*, 68–72. Available online: https://www.met.hu/downloads.php?fn=/metadmin/newspaper/2013/01/ legkor-2012-2.pdf (accessed on 4 May 2023).

38. Mika, J.; Csabai, E.K.; Dobi, I.; Molnár, Z.; Nagy, Z.; Rázsi, A.; Tóth-Tarjányi, Z.; Pajtók-Tari, I. Solar and wind energy resources of the Eger Region. *Hung. Geogr. Bull.* **2014**, *63*, 17–27. [CrossRef]

39. Kovács, E.; Puskás, J.; Pozsgai, A. Positive effects of climate change on the field of Sopron wine-growing region in Hungary. In *Perspectives on Atmospheric Sciences*; Karacostas, T., Bais, A., Nastos, P.T., Eds.; Springer International Publishing: Cham, Switzerland, 2017; pp. 607–613. [CrossRef]

40. Sanchez-Lorenzo, A.; Wild, M.; Brunetti, M.; Guijarro, J.A.; Hakuba, M.Z.; Calbó, J.; Mystakidis, S.; Bartok, B. Reassessment and update of long-term trends in downward surface shortwave radiation over Europe (1939–2012). *J. Geophys. Res. Atmos.* **2015**, *120*, 9555–9569. [CrossRef]

41. Augustine, J.A.; Capotondi, A. Forcing for multidecadal surface solar radiation trends over Northern Hemisphere continents. *J. Geophys. Res. Atmos.* **2022**, *127*, e2021JD036342. [CrossRef]

42. Gulev, S.; Thorne, P.; Ahn, J.; Dentener, F.; Domingues, C.; Gerland, S.; Gong, D.; Kaufman, D.; Nnamchi, H.; Quaas, J.; et al. Changing state of the climate system. In *Climate Change 2021: The Physical Science Basis. Contribution of Working Group I to the Sixth Assessment Report of the Intergovernmental Panel on Climate Change*; Masson-Delmotte, V., Zhai, P., Pirani, A., Connors, S., Péan, C., Berger, S., Caud, N., Chen, Y., Goldfarb, L., Gomis, M., et al., Eds.; Cambridge University Press: Cambridge, UK; New York, NY, USA, 2021; pp. 287–422. [CrossRef]

43. Hersbach, H.; Bell, B.; Berrisford, P.; Hirahara, S.; Horányi, A.; Muñoz-Sabater, J.; Nicolas, J.; Peubey, C.; Radu, R.; Schepers, D.; et al. The ERA5 global reanalysis. *Q. J. R. Meteorol. Soc.* **2020**, *146*, 1999–2049. [CrossRef]

44. Laurila, T.K.; Sinclair, V.A.; Gregow, H. Climatology, variability, and trends in near-surface wind speeds over the North Atlantic and Europe during 1979–2018 based on ERA5. *Int. J. Climatol.* **2021**, *41*, 2253–2278. [CrossRef]

45. Zsilinszki, A.; Dezső, Z.; Bartholy, J.; Pongrácz, R. Synoptic-climatological analysis of high level air flow over the Carpathian Basin. *Időjárás (Q. J. Hung. Meteorol. Serv.)* **2019**, *123*, 19–38. [CrossRef]

46. Gimeno, L.; Eiras-Barca, J.; Durán-Quesada, A.M.; Dominguez, F.; van der Ent, R.; Sodemann, H.; Sánchez-Murillo, R.; Nieto, R.; Kirchner, J.W. The residence time of water vapour in the atmosphere. *Nat. Rev. Earth Environ.* **2021**, *2*, 558–569. [CrossRef]

47. Allan, R.P.; Willett, K.M.; John, V.O.; Trent, T. Global changes in water vapor 1979–2020. *J. Geophys. Res. Atmos.* **2022**, *127*, e2022JD036728. [CrossRef]

48. Spinoni, J.; Antofie, T.; Barbosa, P.; Bihari, Z.; Lakatos, M.; Szalai, S.; Szentimrey, T.; Vogt, J. An overview of drought events in the Carpathian Region in 1961–2010. *Adv. Sci. Res.* **2013**, *10*, 21–32. [CrossRef]

49. Lakatos, M.; Weidinger, T.; Hoffmann, L.; Bihari, Z.; Horváth, A. Computation of daily Penman–Monteith reference evapotranspiration in the Carpathian Region and comparison with Thornthwaite estimates. *Adv. Sci. Res.* **2020**, *16*, 251–259. [CrossRef]

50. Cséplő, A.; Sarkadi, N.; Horváth, A.; Schmeller, G.; Lemler, T. Fog climatology in Hungary. *Időjárás (Q. J. Hung. Meteorol. Serv.)* **2019**, *123*, 241–264. [CrossRef]

51. Ilona, J.; Bartók, B.; Dumitrescu, A.; Cheval, S.; Gandhi, A.; Tordai, A.V.; Weidinger, T. Using long-term historical meteorological data for climate change analysis in the Carpathian region. *Atmosphere* **2022**, *13*, 1751. [CrossRef]

52. Schneider, U.; Finger, P.; Meyer-Christoffer, A.; Rustemeier, E.; Ziese, M.; Becker, A. Evaluating the hydrological cycle over land using the newly-corrected precipitation climatology from the Global Precipitation Climatology Centre (GPCC). *Atmosphere* **2017**, *8*, 52. [CrossRef]

53. Bartholy, J.; Pongrácz, R. Tendencies of extreme climate indices based on daily precipitation in the Carpathian Basin for the 20th century. *Időjárás (Q. J. Hung. Meteorol. Serv.)* **2005**, *109*, 1–20. Available online: https://www.met.hu/ismeret-tar/kiadvanyok/idojaras/index.php?id=238 (accessed on 4 May 2023).

54. Bartholy, J.; Pongrácz, R. Analysis of precipitation conditions for the Carpathian Basin based on extreme indices in the 20th century and climate simulations for 2050 and 2100. *Phys. Chem. Earth* **2010**, *35*, 43–51. [CrossRef]

55. Domonkos, P. Recent precipitation trends in Hungary in the context of larger scale climatic changes. *Nat. Hazards* **2003**, *29*, 255–271. [CrossRef]

56. Lakatos, M.; Szentes, O.; Cindrić Kalin, K.; Nimac, I.; Kozjek, K.; Cheval, S.; Dumitrescu, A.; Irașoc, A.; Stepanek, P.; Farda, A.; et al. Analysis of sub-daily precipitation for the PannEx region. *Atmosphere* **2021**, *12*, 838. [CrossRef]

57. Zólyomi, B.; Kéri, M.; Horváth, F. Spatial and temporal changes in the frequency of climatic year types in the Carpathian Basin. *Coenoses* **1997**, *12*, 33–41. Available online: https://www.jstor.org/stable/43461186 (accessed on 4 May 2023).

58. Szinell, C.S.; Bussay, A.; Szentimrey, T. Drought tendencies in Hungary. *Int. J. Climatol.* **1998**, *18*, 1479–1491. [CrossRef]

59. Gavrilov, M.B.; Radaković, M.G.; Sipos, G.; Mezősi, G.; Gavrilov, G.; Lukić, T.; Basarin, B.; Benyhe, B.; Fiala, K.; Kozák, P.; et al. Aridity in the central and southern Pannonian Basin. *Atmosphere* **2020**, *11*, 1269. [CrossRef]

60. Ilyés, C.; Szűcs, P.; Turai, E. Appearance of climatic cycles and oscillations in Carpathian Basin precipitation data. *Hung. Geogr. Bull.* **2022**, *71*, 21–37. [CrossRef]

61. Rottler, E.; Francke, T.; Bürger, G.; Bronstert, A. Long-term changes in central European river discharge for 1869–2016: Impact of changing snow covers, reservoir constructions and an intensified hydrological cycle. *Hydrol. Earth Syst. Sci.* **2020**, *24*, 1721–1740. [CrossRef]

62. Blöschl, G.; Hall, J.; Parajka, J.; Perdigão, R.A.P.; Merz, B.; Arheimer, B.; Aronica, G.T.; Bilibashi, A.; Bonacci, O.; Borga, M.; et al. Changing climate shifts timing of European floods. *Science* **2017**, *357*, 588–590. [CrossRef]

63. Hall, J.; Arheimer, B.; Aronica, G.T.; Bilibashi, A.; Boháč, M.; Bonacci, O.; Borga, M.; Burlando, P.; Castellarin, A.; Chirico, G.B.; et al. A European Flood Database: Facilitating comprehensive flood research beyond administrative boundaries. *Proc. Int. Assoc. Hydrol. Sci.* **2015**, *370*, 89–95. [CrossRef]

64. Kundzewicz, Z.W.; Pińskwar, I.; Brakenridge, G.R. Changes in river flood hazard in Europe: A review. *Hydrol. Res.* **2017**, *49*, 294–302. [CrossRef]

65. Kettner, A.; Brakenridge, G.R.; Schumann, G.J.P.; Shen, X. Chapter 7: DFO—Flood Observatory. In *Earth Observation for Flood Applications*; Schumann, G.J.P., Ed.; Earth Observation; Elsevier: Amsterdam, The Netherlands, 2021; pp. 147–164. [CrossRef]

66. Blöschl, G.; Hall, J.; Viglione, A.; Perdigão, R.A.P.; Parajka, J.; Merz, B.; Lun, D.; Arheimer, B.; Aronica, G.T.; Bilibashi, A.; et al. Changing climate both increases and decreases European river floods. *Nature* **2019**, *573*, 108–111. [CrossRef]

67. Bertola, M.; Viglione, A.; Lun, D.; Hall, J.; Blöschl, G. Flood trends in Europe: Are changes in small and big floods different? *Hydrol. Earth Syst. Sci.* **2020**, *24*, 1805–1822. [CrossRef]

68. Berghuijs, W.R.; Allen, S.T.; Harrigan, S.; Kirchner, J.W. Growing spatial scales of synchronous siver flooding in Europe. *Geophys. Res. Lett.* **2019**, *46*, 1423–1428. [CrossRef]

69. Kemter, M.; Merz, B.; Marwan, N.; Vorogushyn, S.; Blöschl, G. Joint trends in flood magnitudes and spatial extents across Europe. *Geophys. Res. Lett.* **2020**, *47*, e2020GL087464. [CrossRef] [PubMed]

70. Pekarova, P.; Skoda, P.; Miklanek, P.; Halmova, D.; Pekar, J. Detection of changes in flow variability of the upper Danube between 1876–2006. *IOP Conf. Ser. Earth Environ. Sci.* **2008**, *4*, 012028. [CrossRef]

71. Nováky, B.; Bálint, G. Shifts and modification of the hydrological regime under climate change in Hungary. In *Climate Change—Realities, Impacts Over Ice Cap, Sea Level and Risks*; Singh, B.R., Ed.; InTechOpen: London, UK, 2013; pp. 163–190. [CrossRef]

72. Konecsny, K.; Nagy, Z. Similarities and differences of the hydrological extremes on the Duna/Danube and Tisza/Tisa rivers (1921–2012). In *Air and Water Components of the Environment*; Serban, G., Horváth, C., Holobaca, I., Batinas, R., Tudose, T., Croitoru, A., Eds.; Cluj University Press: Cluj-Napoca, Romania, 2014; pp. 134–141. Available online: http://aerapa.conference.ubbcluj.ro/2014/PDF/18-Konecsny-Nagy.pdf (accessed on 4 May 2023).

73. Tadić, L.; Tamás, E.A.; Mihaljević, M.; Janjić, J. Potential climate impacts of hydrological alterations and discharge variabilities of the Mura, Drava, and Danube rivers on the natural resources of the MDD UNESCO Biosphere Reserve. *Climate* **2022**, *10*, 139. [CrossRef]

74. Illés, Z.; Nagy, L. Effect of climate change on earthworks of infrastructure: Statistical evaluation of the cause of dike pavement cracks. *Geoenviron. Disasters* **2022**, *9*, 20. [CrossRef]

75. Nagy, L. Dike failures in the Carpathian Basin. *Sci. Secur.* **2022**, *2*, 510–518. [CrossRef]

76. Merz, R.; Blöschl, G. A process typology of regional floods. *Water Resour. Res.* **2003**, *39*, 1340. [CrossRef]

77. Blöschl, G.; Bierkens, M.F.; Chambel, A.; Cudennec, C.; Destouni, G.; Fiori, A.; Kirchner, J.W.; McDonnell, J.J.; Savenije, H.H.; Sivapalan, M.; et al. Twenty-three unsolved problems in hydrology (UPH)—A community perspective. *Hydrol. Sci. J.* **2019**, *64*, 1141–1158. [CrossRef]

78. Hall, J.; Arheimer, B.; Borga, M.; Brázdil, R.; Claps, P.; Kiss, A.; Kjeldsen, T.R.; Kriaučiūnienė, J.; Kundzewicz, Z.W.; Lang, M.; et al. Understanding flood regime changes in Europe: A state-of-the-art assessment. *Hydrol. Earth Syst. Sci.* **2014**, *18*, 2735–2772. [CrossRef]

79. Hall, J.; Blöschl, G. Spatial patterns and characteristics of flood seasonality in Europe. *Hydrol. Earth Syst. Sci.* **2018**, *22*, 3883–3901. [CrossRef]

80. Borsos, B.; Sendzimir, J. The Tisza river: Managing a lowland river in the Carpathian Basin. In *Riverine Ecosystem Management: Science for Governing Towards a Sustainable Future*; Schmutz, S., Sendzimir, J., Eds.; Springer International Publishing: Cham, Switzerland, 2018; pp. 541–560. [CrossRef]

81. Press, W.H.; Rybicki, G.B. Fast algorithm for spectral analysis of unevenly sampled data. *Astrophys. J.* **1989**, *338*, 277–280. Available online: https://adsabs.harvard.edu/full/1989ApJ...338..277P (accessed on 4 May 2023). [CrossRef]

82. VanderPlas, J.T. Understanding the Lomb–Scargle Periodogram. *Astrophys. J. Suppl. Ser.* **2018**, *236*, 16. [CrossRef]

83. Virtanen, P.; Gommers, R.; Oliphant, T.E.; Haberland, M.; Reddy, T.; Cournapeau, D.; Burovski, E.; Peterson, P.; Weckesser, W.; Bright, J.; et al. SciPy 1.0: Fundamental algorithms for scientific computing in Python. *Nat. Methods* **2020**, *17*, 261–272. [CrossRef] [PubMed]

84. Taylor, R.G.; Scanlon, B.; Döll, P.; Rodell, M.; van Beek, R.; Wada, Y.; Longuevergne, L.; Leblanc, M.; Famiglietti, J.S.; Edmunds, M.; et al. Ground water and climate change. *Nat. Clim. Chang.* **2013**, *3*, 322–329. [CrossRef]

85. Reinecke, R.; Müller Schmied, H.; Trautmann, T.; Andersen, L.S.; Burek, P.; Flörke, M.; Gosling, S.N.; Grillakis, M.; Hanasaki, N.; Koutroulis, A.; et al. Uncertainty of simulated groundwater recharge at different global warming levels: A global-scale multi-model ensemble study *Hydrol. Earth Syst. Sci.* **2021**, *25*, 787–810. [CrossRef]

86. Bogardi, J.J.; Fekete, B.M. Water: A unique phenomenon and resource. In *Handbook of Water Resources Management: Discourses, Concepts and Examples*; Bogardi, J.J., Gupta, J., Nandalal, K.D.W., Salamé, L., van Nooijen, R.R., Kumar, N., Tingsanchali, T., Bhaduri, A., Kolechkina, A.G., Eds.; Springer International Publishing: Cham, Switzerland, 2021; pp. 9–40. [CrossRef]

87. Allan, R.P.; Barlow, M.; Byrne, M.P.; Cherchi, A.; Douville, H.; Fowler, H.J.; Gan, T.Y.; Pendergrass, A.G.; Rosenfeld, D.; Swann, A.L.S.; et al. Advances in understanding large-scale responses of the water cycle to climate change. *Ann. N. Y. Acad. Sci.* **2020**, *1472*, 49–75. [CrossRef]

88. Xanke, J.; Liesch, T. Quantification and possible causes of declining groundwater resources in the Euro-Mediterranean region from 2003 to 2020. *Hydrogeol. J.* **2022**, *30*, 379–400. [CrossRef]

89. Chao, N.; Luo, Z.; Wang, Z.; Jin, T. Retrieving groundwater depletion and drought in the Tigris-Euphrates Basin between 2003 and 2015. *Groundwater* **2018**, *56*, 770–782. [CrossRef]

90. Frappart, F.; Ramillien, G. Monitoring groundwater storage changes using the Gravity Recovery and Climate Experiment (GRACE) satellite mission: A review. *Remote Sens.* **2018**, *10*, 829. [CrossRef]

91. Szalai, J. Changes in groundwater-table on the Great Hungarian Plain (in Hungarian). In *Environmental changes and the Great Hungarian Plain (in Hungarian)*; Rakonczai, J., Ed.; Nagyalföld Alapítvány (Great Plain Foundation): Békéscsaba, Hungary, 2011; pp. 99–110. Available online: https://acta.bibl.u-szeged.hu/62614/ (accessed on 4 May 2023).

92. Rakonczai, J. Effects and consequences of global climate change in the Carpathian Basin. In *Climate Change—Geophysical Foundations and Ecological Effects*; Blanco, J.A., Kheradmand, H., Eds.; IntechOpen: Rijeka, Croatia, 2011; pp. 297–322. [CrossRef]

93. Rakonczai, J.; Fehér, Z. The role of climate change in the temporal changes of the groundwater resources of the Hungarian Great Plain (in Hungarian). *Hidrológiai Közlöny (Hung. J. Hydrol.)* **2015**, *95*, 1–15. Available online: https://library.hungaricana.hu/hu/view/HidrologiaiKozlony_2015/?pg=2&layout=s (accessed on 4 May 2023).

94. Garamhegyi, T.; Kovács, J.; Pongrácz, R.; Tanos, P.; Hatvani, I.G. Investigation of the climate-driven periodicity of shallow groundwater level fluctuations in a Central-Eastern European agricultural region. *Hydrogeol. J.* **2018**, *26*, 677–688. [CrossRef]

95. Garamhegyi, T.; Hatvani, I.G.; Szalai, J.; Kovács, J. Delineation of hydraulic flow regime areas based on the statistical analysis of semicentennial shallow groundwater table time series. *Water* **2020**, *12*, 828. [CrossRef]

96. Liebe, P.; Kumánovics, G.; Rózsa, A.; Szongoth, G.; Tahy, A.; Szöllősi-Nagy, A.; Csiszár, E.; Pump, J.; Lénárt, L. Problems related to wells in the field of sustainable management of underground water resources and water protection (in Hungarian). *Vízügyi Közlöny (Hung. Water Bull.)* **2021**, *1022*, 33–67. Available online: https://library.hungaricana.hu/hu/view/VizugyiKozlemenyek_2021/?pg=206&layout=s (accessed on 4 May 2023).

97. Tran, H.Q.; Fehér, Z.Z.; Túri, N.; Rakonczai, J. Climate change as an environmental threat on the central plains of the Carpathian Basin based on regional water balances. *Geogr. Pannonica* **2022**, *26*, 184–199. [CrossRef]

98. Trásy, B.; Kovács, J.; Hatvani, I.; Havril, T.; Németh, T.; Scharek, P.; Szabó, C. Assessment of the interaction between surface- and groundwater after the diversion of the inner delta of the River Danube (Hungary) using multivariate statistics. *Anthropocene* **2018**, *22*, 51–65. [CrossRef]

99. Kubacki, M.; Tran, H. Non-iterative partitioned methods for uncoupling evolutionary groundwater-surface water flows. *Fluids* **2017**, *2*, 3. [CrossRef]

100. Beliaev, A.; Krichevets, G. Qualitative effects of hydraulic conductivity distribution on groundwater flow in heterogeneous soils. *Fluids* **2018**, *3*, 102. [CrossRef]

101. Syvitski, J.; Ángel, J.R.; Saito, Y.; Overeem, I.; Vörösmarty, C.J.; Wang, H.; Olago, D. Earth's sediment cycle during the Anthropocene. *Nat. Rev. Earth Environ.* **2022**, *3*, 179–196. [CrossRef]

102. Kalocsa, B.; Zsuffa, I. Changes in the water level of the Hungarian section of the Danube (in Hungarian). *Hidrológiai Közlöny (Hung. J. Hydrol.)* **1997**, *77*, 183–192. Available online: https://library.hungaricana.hu/hu/view/HidrologiaiKozlony_1997/?pg=188&layout=s (accessed on 4 May 2023).

103. Goda, L.; Kalocsa, B.; Tamás, E.A. River bed erosion on the Hungarian section of the Danube. *J. Environ. Sci. Sustain. Soc.* **2007**, *1*, 47–54. [CrossRef]

104. Habersack, H.; Jäger, E.; Hauer, C. The status of the Danube River sediment regime and morphology as a basis for future basin management. *Int. J. River Basin Manag.* **2013**, *11*, 153–166. [CrossRef]

105. Habersack, H.; Hein, T.; Stanica, A.; Liska, I.; Mair, R.; Jäger, E.; Hauer, C.; Bradley, C. Challenges of river basin management: Current status of, and prospects for, the River Danube from a river engineering perspective. *Sci. Total Environ.* **2016**, *543*, 828–845. [CrossRef] [PubMed]

106. Bonacci, O.; Oskoruš, D. The changes in the lower Drava River water level, discharge and suspended sediment regime. *Environ. Earth. Sci.* **2010**, *59*, 1661–1670. [CrossRef]

107. Tomsett, C.; Leyland, J. Remote sensing of river corridors: A review of current trends and future directions. *River Res. Appl.* **2019**, *35*, 779–803. [CrossRef]

108. Lewicka, O.; Specht, M.; Stateczny, A.; Specht, C.; Dardanelli, G.; Brčić, D.; Szostak, B.; Halicki, A.; Stateczny, M.; Widźgowski, S. Integration data model of the bathymetric monitoring system for shallow waterbodies using UAV and USV platforms. *Remote Sens.* **2022**, *14*, 4075. [CrossRef]

109. Rentier, E.; Cammeraat, L. The environmental impacts of river sand mining. *Sci. Total Environ.* **2022**, *838*, 155877. [CrossRef]

110. Pandey, S.; Kumar, G.; Kumari, N.; Pandey, R. Assessment of causes and impacts of sand mining on river ecosystem. In *Hydrogeochemistry of Aquatic Ecosystems*; John Wiley & Sons: Hoboken, NJ, USA, 2023; Chapter 16, pp. 357–379. [CrossRef]

111. Borics, G.; Lukács, B.A.; Grigorszky, I.; Zsolt, L.N.; László, G.-T.; Sándor, S.; Görgényi, J.; Várbíró, G. Phytoplankton-based shallow lake types in the Carpathian basin: Steps towards a bottom-up typology. *Fundam. Appl. Limnol.* **2014**, *184*, 23–34. [CrossRef]

112. Kiss, A. *Floods and Long-Term Water-Level Changes in Medieval Hungary*; Springer International Publishing: Cham, Switzerland, 2019; pp. 1–896. [CrossRef]

113. Kutics, K. Evolution of water quality of Lake Balaton. *Ecocycles* **2019**, *5*, 44–73. [CrossRef]

114. Kutics, K.; Kravinszkaja, G. Lake Balaton hydrology and climate change. *Ecocycles* **2020**, *6*, 88–97. [CrossRef]

115. Kutics, K. Peculiarities and problems of shallow lakes (in Hungarian). *Acta Scientiarum Socialium* **2013**, *39*, 11–34. Available online: http://journal.ke.hu/index.php/asc/article/view/313 (accessed on 4 May 2023).

116. Nagy-Szijártó, B.C.; Szalmáné Csete, M. Investigating sustainable settlement development in the Lake Velence area. (In Hungarian). *Modern Geográfia* **2023**, *18*, 1–26. [CrossRef]

117. Kiss, A. Historical climatology in Hungary: Role of documentary evidence in the study of past climates and hydrometeorological extremes. *Időjárás (Q. J. Hung. Meteorol. Serv.)* **2009**, *113*, 315–339. Available online: https://www.met.hu/ismeret-tar/kiadvanyok/idojaras/index.php?id=146 (accessed on 4 May 2023).

118. Lóczy, D.; Dezső, J.; Gyenizse, P.; Czigány, S.; Tóth, G. Oxbow lakes: Hydromorphology. In *The Drava River: Environmental Problems and Solutions*; Lóczy, D., Ed.; Springer International Publishing: Cham, Switzerland, 2019; pp. 177–198. [CrossRef]

119. Pálfai, I., Ed. *Oxbow Lakes in Hungary (Magyarország Holtágai, in Hungarian)*; Ministry of Transport, Public Works and Water Management: Budapest, Hungary, 2001; pp. 1–232. ISBN 963 009156 9.

120. Borics, G.; Ács, É.; Boda, P.; Boros, E.; Erős, T.; Grigorszky, I.; Kiss, K.T.; Lengyel, S.; Nagy, M.R.; Somogyi, B.; et al. Water bodies in Hungary—An overview of their management and present state (in Hungarian). *Hidrológiai Közlöny (Hung. J. Hydrol.)* **2016**, *96*, 57–67. Available online: https://library.hungaricana.hu/hu/view/HidrologiaiKozlony_2016/?pg=232&layout=s (accessed on 4 May 2023).

121. Singh, K.P.; Stall, J.B. Derivation of base flow recession curves and parameters. *Water Res. Res.* **1971**, *7*, 292–303. [CrossRef]

122. Wittenberg, H. Baseflow recession and recharge as nonlinear storage processes. *Hydrol. Proc.* **1999**, *13*, 715–726. [CrossRef]
123. Guo, J. Application of general unit hydrograph model for baseflow separation from rainfall and streamflow data. *J. Hydrol. Eng.* **2022**, *27*, 04022027. [CrossRef]
124. Giorgi, F. Thirty years of regional climate modeling: Where are we and where are we going next? *J. Geophys. Res. Atmos.* **2019**, *124*, 5696–5723. [CrossRef]
125. Carter, J.; Leeson, A.; Orr, A.; Kittel, C.; van Wessem, J.M. Variability in Antarctic surface climatology across regional climate models and reanalysis datasets. *Cryosphere* **2022**, *16*, 3815–3841. [CrossRef]
126. Saharwardi, M.S.; Kumar, P. Future drought changes and associated uncertainty over the homogenous regions of India: A multimodel approach. *Int. J. Climatol.* **2022**, *42*, 652–670. [CrossRef]
127. Gallardo, V.; Sánchez-Gómez, E.; Riber, E.; Boé, J.; Terray, L. Evolution of high-temperature extremes over the main Euro-Mediterranean airports. *Clim. Dyn.* **2023**, *online first*. [CrossRef]
128. Hakala, K.; Addor, N.; Teutschbein, C.; Vis, M.; Dakhlaoui, H.; Seibert, J. Hydrological modeling of climate change impacts. In *Encyclopedia of Water: Science, Technology, and Society*; Maurice, P., Ed.; John Wiley & Sons, Inc.: Hoboken, NJ, USA, 2019; pp. 2337–22356. [CrossRef]
129. Gelybó, G.; Tóth, E.; Farkas, C.; Horel, A.; Kása, I.; Bakacsi, Z. Potential impacts of climate change on soil properties. *Agrokémia Talajtan (Agrochem. Soil Sci.)* **2018**, *67*, 121–141. [CrossRef]
130. Meyer, J.; Neuper, M.; Mathias, L.; Zehe, E.; Pfister, L. Atmospheric conditions favouring extreme precipitation and flash floods in temperate regions of Europe. *Hydrol. Earth Syst. Sci.* **2022**, *26*, 6163–6183. [CrossRef]
131. Steirou, E.; Gerlitz, L.; Sun, X.; Apel, H.; Agarwal, A.; Totz, S.; Merz, B. Towards seasonal forecasting of flood probabilities in Europe using climate and catchment information. *Sci. Rep.* **2022**, *12*, 13514. [CrossRef]
132. Burrell, B.C.; Beltaos, S.; Turcotte, B. Effects of climate change on river-ice processes and ice jams. *Int. J. River Basin Manag.* **2022**, *online first*. [CrossRef]
133. Huokuna, M.; Morris, M.; Beltaos, S.; Burrell, B.C. Ice in reservoirs and regulated rivers. *Int. J. River Basin Manag.* **2022**, *20*, 1–16. [CrossRef]
134. Lindenschmidt, K.-E.; Alfredsen, K.; Carstensen, D.; Choryński, A.; Gustafsson, D.; Halicki, M.; Hentschel, B.; Karjalainen, N.; Kögel, M.; Kolerski, T.; et al. Assessing and mitigating ice-jam flood hazards and risks: A European perspective. *Water* **2023**, *15*, 76. [CrossRef]